AIP | Physics of Fluids

Can flexibility help you float?

L. J. Burton and J. W. M. Bush

Citation: Phys. Fluids **24**, 101701 (2012); doi: 10.1063/1.4757121
View online: http://dx.doi.org/10.1063/1.4757121
View Table of Contents: http://pof.aip.org/resource/1/PHFLE6/v24/i10
Published by the American Institute of Physics.

Can flexibility help you float?

L. J. Burton[1,a)] and J. W. M. Bush[2]
[1]*Department of Mechanical Engineering, Massachusetts Institute of Technology, 77 Massachusetts Avenue, Cambridge, Massachusetts 02139-4307, USA*
[2]*Department of Mathematics, Massachusetts Institute of Technology, 77 Massachusetts Avenue, Cambridge, Massachusetts 02139-4307, USA*

(Received 27 June 2012; accepted 14 September 2012; published online 1 October 2012)

We consider the role of flexibility in the weight-bearing characteristics of bodies floating at an interface. Specifically, we develop a theoretical model for a two-dimensional thin floating plate that yields the maximum stable plate load and optimal stiffness for weight support. Plates small relative to the capillary length are primarily supported by surface tension, and their weight-bearing potential does not benefit from flexibility. Above a critical size comparable to the capillary length, flexibility assists interfacial flotation. For plates on the order of and larger than the capillary length, deflection from an initially flat shape increases the force resulting from hydrostatic pressure, allowing the plate to support a greater load. In this large plate limit, the shape that bears the most weight is a semicircle, which displaces the most fluid above the plate for a fixed plate length. Exact results for maximum weight-bearing plate shapes are compared to analytic approximations made in the limits of large and small plate sizes. The value of flexibility for floating to a number of biological organisms is discussed in light of our study. © *2012 American Institute of Physics*. [http://dx.doi.org/10.1063/1.4757121]

Introduction: In his treatise *On Floating Bodies*, Archimedes[1] examined the stability of objects wholly or partially submerged in a fluid. He surmised that if an object is less dense than the suspending fluid, it will partially project above the surface, displacing a volume of fluid with a weight equal to its own. This proposition, commonly known as Archimedes' principle, is true for large objects, but neglects capillary effects that arise at small scales, specifically, at scales small relative to the capillary length. Keller[2] generalized Archimedes' principle to small floating bodies by showing that the vertical force from surface tension is equal to the weight of liquid displaced by the meniscus. We here extend this class of problems by elucidating the role of flexibility in interfacial flotation.

Many biological organisms that float, such as hydrophytes (e.g., water lilies) and water walking insects,[3] are not entirely rigid. There are several reasons for organisms to be flexible, including decreased weight and increased robustness when subjected to external forces.[4] *Hydrophytics* are aquatic plants rooted in the soil. During times of flood, their petals bend and close, thereby protecting their genetic material in response to increasing hydrostatic pressure.[5] Flexibility is exploited by several creatures that reside at the water surface, both individually and collectively. The insect *Anurida* attracts others of its kind by bending its back and deforming the interface, so that a colony can behave like a self-assembling raft.[3] Other such living rafts may form from assemblages of mosquito eggs[6] or whirligig beetles.[7] Though individual ants flounder at the interface, ant rafts, comprised of thousands of individuals, are able to stay afloat for months in the flood-prone rain forests of Brazil.[8] Might such interfacial organisms, as individuals or a collective, exploit flexibility to support a greater load?

The role of flexibility in interfacial flotation has only been considered relatively recently. Vella *et al.*[9] examined the weight-bearing characteristics of a raft composed of thin rigid strips. Several

a)Electronic mail: lisab@mit.edu.

studies have been inspired by the legs of water-walking insects, including examinations of the flexure of a floating cylindrical rod forced at one end[10] and the deformation of a thin sheet pressed against a liquid interface.[11] Ji *et al.*[12] modeled a water strider leg as a cantilever beam and compared the results of their predictions to experiments with flexible fibers. Zheng *et al.*[13] considered the relative importance of water strider leg deformation and surface texture in weight bearing. Floating hydrophobic rods of various cross sectional shapes were studied by Liu *et al.*[14] Reis *et al.*[5] computed the shape of a floating two-dimensional strip subjected to a point force at its center. Consideration was given to the balance between the work done by hydrostatic forces and bending energy of the strip while the contribution of surface tension to flotation was neglected. Vella[6] demonstrated that rafts with finite bending stiffness can support greater loads than their rigid counterparts, and verified these theoretical predications with an experimental study of floating rafts of self-assembled thin strips. For floating plates, one expects surface tension forces to dominate forces resulting from hydrostatic pressure for plates much smaller than the capillary length. The equilibrium shape of such small plates will thus have little influence on the maximum load the plate can support, which will be prescribed by its edge length. Conversely, large plates will be supported predominantly by hydrostatic pressure on the plate; consequently, maximum loads will be supported by plates that displace the most fluid.

In "Flotation of hinged plates," we consider a two-dimensional hinged plate with a torsion spring, so that bending is permitted only at a single point. To determine whether flexibility is advantageous, we derive the maximum load (specifically, the maximum plate density) that can be supported. The effect of increasing spring stiffness on the equilibrium plate shape is determined. These results are useful in developing intuition for "Continuously deformable plates," where we generalize our model to the case of continuously deformable plates. The cases of small, large, and intermediate sized plates are considered, and plate configurations and approximations for the optimal spring stiffness (those capable of supporting the greatest load) are derived. Our results are reviewed in "Discussion," where their bearing on the form of some aquatic plants is discussed.

Flotation of hinged plates: Here we examine the simplified case of two rigid plates connected by a torsion spring. Consider the two-dimensional geometry in which two infinitely long rigid plates of width b and thickness t (such that $b \gg t$) are connected by a torsion spring with spring constant per unit width K_s (Fig. 1(a)). The air density is assumed to be negligible relative to that of the liquid, ρ, and the solid plate, ρ_s. The capillary length is defined as $\ell_c^2 = \sigma/\rho g$ where σ is surface tension and g gravity, and the elastocapillary length is $\ell_{ec}^2 = K_s/\sigma$. The hinge angle is α and the interfacial slope ϕ is related to the plate edge depth by $h = \ell_c\sqrt{2-2\cos\phi}$. The plate edge depth, h, is the distance from the undisturbed interface to the plate's outer edge and must be less than or equal to two capillary lengths; otherwise, the meniscus will collapse. The contact angle between the plate and the interface may take on a range of values due to the possibility of pinning at the plate edge. To increase the load on the plate uniformly, its density ρ_s is increased. As the load increases, the plate will sink and, depending on the magnitude of K_s, bend. Beyond some maximum load (to be determined), the plate will sink. Our approach extends the work of Vella *et al.*[9] through consideration of the torsion spring, which imposes an energetic penalty to flexure.

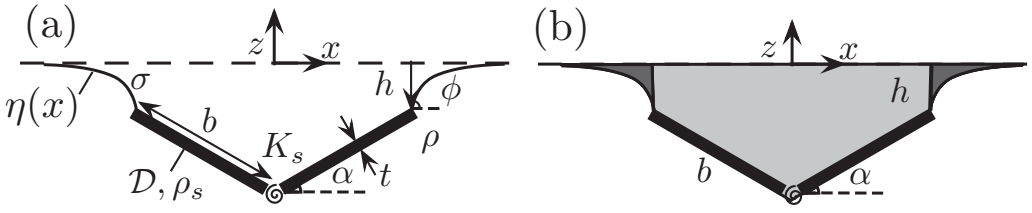

FIG. 1. (a) Two-dimensional geometry of the hinged two-plate configuration. Two plates, each of length b, thickness t, and density ρ_s are connected by a torsion spring with spring constant K_s. The outer plate edges are a distance h below the undisturbed interface. Flexure causes the plates to lie at an angle α with respect to the horizontal. The density of the liquid is ρ and the surface tension is σ. (b) Dark shaded regions show fluid displaced above the meniscus, whose weight is equal to the vertical component of surface tension, while the light shaded region shows the volume of fluid displaced above the plate.

Energetics: We seek to identify the configuration parameters (α, h) that minimize the total system energy. The potential energy associated with the work done on the system by external forces is V. We express V as the combination of work done by: hydrostatic pressure on the interface, $E_{\mathrm{H,\,i}}$, hydrostatic pressure on the plate, $E_{\mathrm{H,\,p}}$, gravity on the plate, E_{p}, and surface tension on the plate, E_σ,

$$V = E_{\mathrm{H,i}} + E_{\mathrm{H,p}} + E_{\mathrm{p}} + E_\sigma. \tag{1}$$

We define U to be the combination of surface or "free" energy, S, and the potential energy stored in the torsion spring, $E_{\mathrm{s}} = K_s(2\alpha)^2/2$,

$$U = S + E_{\mathrm{s}}. \tag{2}$$

A body will deform to the configuration that minimizes the system's total potential energy, $\Pi = U - V$. We thus identify the configuration parameters that result in zero variation in total potential energy, $\delta\Pi = \delta U - \delta V = 0$, or that correspond to a stationary point in the energy landscape.[15] The variation in the energy terms is

$$\delta V = \rho g \int \eta(x) dx \delta\epsilon + \rho g \left(\left(2bh\cos\alpha + b^2\cos\alpha\sin\alpha\right)\delta h + \left(\frac{b^3}{3}\sin\alpha + b^2 h\right)\delta\alpha \right) \ldots$$
$$- \rho_s g t \left(2b\delta h + b^2\cos\alpha\delta\alpha\right) + 2\sigma\left(\sin\phi\delta h + b\left(\sin\phi\cos\alpha - \cos\phi\sin\alpha\right)\delta\alpha\right), \tag{3}$$

$$\delta U = \sigma\delta\ell + 4K_s\alpha\delta\alpha = \sigma\int \nabla\cdot\vec{n} dx\delta\epsilon + 4K_s\alpha\delta\alpha, \tag{4}$$

where $z = \eta(x)$ is the known equation of the interface and $\delta\epsilon$ is the incremental displacement of the interface. The outward vector normal to the interface is $\vec{n}$ and $\delta\ell$ is the incremental change in arc length along the meniscus. We describe the plate configuration by parameters α and h and set the variation in energy with each parameter to zero. Two equations must be satisfied for static equilibrium:

$$\frac{\delta\Pi}{\delta h} = -\rho g\left(2bh\cos\alpha + b^2\cos\alpha\sin\alpha\right) + 2b\rho_s g t - \sigma h\sqrt{4\ell_c^2 - h^2} = 0, \tag{5}$$

$$\frac{\delta\Pi}{\delta\alpha} = 4K_s\alpha - \rho g\left(\frac{b^3\sin\alpha}{3} + b^2 h\right) + \rho_s g t b^2\cos\alpha$$
$$+ \sigma b\left(-h\sqrt{4\ell_c^2 - h^2}\cos\alpha + \left(2\ell_c^2 - h^2\right)\sin\alpha\right) = 0. \tag{6}$$

These equations express, respectively, the force balance on the plate and the balance of torques about the torsion spring. The surface energy and the gravitational potential energy associated with the interface cancel precisely, as follows from application of the Young-Laplace equation at the interface, $\rho g\eta(x) = -\sigma\nabla\cdot\vec{n}$: along the meniscus, the curvature, and hydrostatic pressures are in balance.

Buckingham's theorem indicates five dimensionless groups, defined in Table I. The dimensionless plate stiffness is related to the ratio of the elastocapillary length and the capillary length by $k_s = (\ell_{ec}/\ell_c)^2$. Thus, for a fixed capillary length, the plate shape is prescribed by either the plate stiffness or elastocapillary length. The Bond number, $Bo = (b/\ell_c)^2 = \beta^2$, is of particular interest. We focus on the two extremes of plate size; henceforth, "small" and "large" plates correspond to the

TABLE I. Relevant dimensionless groups.

Plate half-length	b	$\beta = \frac{b}{\ell_c}$	Spring constant	$k_s = \frac{K_s}{\rho g\ell_c^3} = \frac{\ell_{ec}^2}{\ell_c^2}$
Plate thickness	t	$\tau = \frac{t}{\ell_c}$	Plate stiffness	$\Lambda = \frac{EI}{\rho g\ell_c^4} = \frac{\ell_{ec}^2}{\ell_c^2}$
Plate edge depth	h	$H = \frac{h}{\ell_c}$	Load	$\mathcal{D} = D\tau = \frac{\rho_s - \rho}{\rho}\tau$
Density	$\rho_s - \rho$	$D = \frac{\rho_s - \rho}{\rho}$	Bond number	$Bo = \frac{b^2\rho g}{\sigma} = \frac{b^2}{\ell_c^2} = \beta^2$

limits of $\beta \ll 1$ and $\beta \gg 1$, respectively. Non-dimensionalizing (5) yields

$$2\beta\mathcal{D} = 2\beta H\cos\alpha + \beta^2\cos\alpha\sin\alpha + H\sqrt{4-H^2}, \tag{7}$$

$$4k_s\alpha + \mathcal{D}\beta^2\cos\alpha = \frac{\beta^3}{3}\sin\alpha + \beta^2 H + \beta\cos\alpha H\sqrt{4-H^2} + \beta\sin\alpha\left(H^2-2\right). \tag{8}$$

Equation (7) expresses the dimensionless force balance, from which the generalization of Archimedes' principle emerges:[2] the weight of the plate is equal to that of the fluid displaced above both the meniscus and the plate (Fig. 1(b)). Equation (8) expresses the dimensionless torque balance: the torques resulting from hydrostatic pressure and surface tension are resisted by the spring torque and that resulting from the weight of the plate.

We seek the configuration parameters that result in the maximum load $\mathcal{D}_{\max}$ for a fixed β, along with the optimal plate stiffness k_s^* necessary to reach that configuration. The problem is expressed as an optimization problem,

$$\max_{\alpha,H,k_s} \mathcal{D}(\beta,\alpha,H,k_s) \quad \text{s.t.} \quad \Sigma F(\beta,\alpha,H,\mathcal{D}) = 0, \quad \Sigma\tau(\beta,\alpha,H,\mathcal{D},k_s) = 0. \tag{9}$$

From the objective function and first constraint, the configuration parameters are determined analytically as a function of plate size,

$$H_{\max\mathcal{D}} = \frac{2\left(\sqrt{2}+\beta\right)}{\sqrt{4+2\sqrt{2}\beta+\beta^2}}, \quad \alpha_{\max\mathcal{D}} = \arccos\left(\sqrt{\frac{1}{2}+\frac{8+\beta^2\left(-2+\sqrt{2}\beta\right)}{16+\beta^4}}\right) \tag{10}$$

and substituted into (7) to find the maximum load,

$$\mathcal{D}_{\max} = \frac{\beta}{4}+\sqrt{2}+\frac{1}{\beta}. \tag{11}$$

Figures 2(a) and 2(b) illustrate the dependence of the optimal configuration parameters and density on the plate size. The optimal stiffness k_s^* for a given plate size is found by solving (8) assuming the optimal configuration defined in (10). The relationship between plate size and optimal stiffness is shown in Fig. 2(c).

The behavior in the limits of large and small plates is deduced by considering the dominant terms in (7) and (8). For small plates, the force and torque balances become, respectively: $2\beta\mathcal{D} \approx H\sqrt{4-H^2}$ and $4k_s\alpha + \mathcal{D}\beta^2\cos\alpha \approx \beta\cos\alpha H\sqrt{4-H^2} + \beta\sin\alpha\left(H^2-2\right)$. The force and torque balances are prescribed by contributions from the spring, the weight of the plate, and the surface tension. It is clear that $H = \sqrt{2}$ maximizes the vertical component of surface tension acting

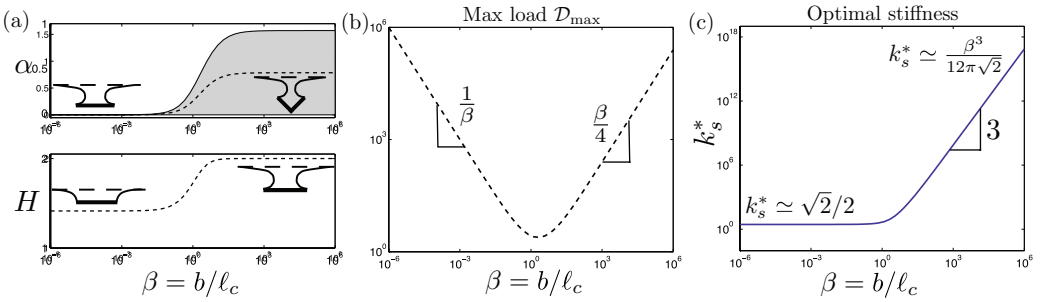

FIG. 2. (a) Plate hinge angle α and plate edge depth H that maximize load as a function of plate size $\beta = b/\ell_c$. Small plates maximize the surface tension force by sinking to a depth $H = \sqrt{2}$ while large plates maximize fluid displaced by assuming a plate tilt angle $\alpha = \pi/4$. The shaded area represents the region where bending allows the plate to support a greater load than a flat plate of the same size. (b) Maximum load as a function of dimensionless plate size, $\beta = b/\ell_c$. (c) Optimal stiffness k_s^* (specifically, that which bears the most weight) as a function of plate size. The optimal stiffness for large plates depends on size because the dominant terms in the force and torque balances are due to hydrostatic pressure and increase with plate size. The weight of small plates is supported primarily by surface tension, thus the independence of k_s^* on plate size for $\beta \ll 1$.

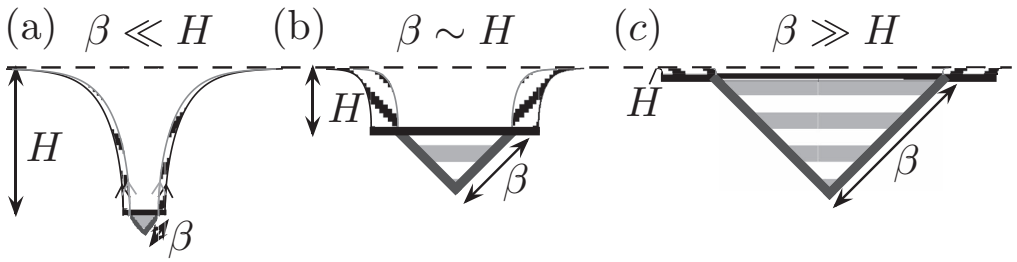

FIG. 3. The dependence on plate size. Horizontal striped regions represent fluid displaced by the bent plate only. Diagonal striped regions indicate where only the flat plate displaces fluid. (a) For plates much smaller than a capillary length, the plate edge depth H determines the amount of fluid displaced (accurate to $\mathcal{O}(\beta/H)$), and therefore the maximum plate load. Bending such small plates decreases the total fluid displaced by narrowing the column of fluid displaced above the plate, thereby diminishing its weight-bearing characteristics. (b) Bending is advantageous for plates on the order of the capillary length if more fluid is displaced by bending than is lost by narrowing the fluid column above the plate. (c) Large plates displace significantly more fluid by bending: flexibility thus enables them to bear greater loads.

on the plate, in accord with Fig. 2(a). This depth also maximizes the liquid displaced, consistent with the generalization of Archimedes' principle.[2] We see from Fig. 3(a) that for small plates ($\beta \ll 1$), bending only serves to reduce the column of fluid displaced above the plate, decreasing the load the plate can bear. In the limit of $\beta \to 0$, the optimal hinge angle is zero and $k_s^* = \sqrt{2}/2$, as may be deduced by considering higher order terms. For these conditions, the maximum load is $\mathcal{D}_{\max} \sim 1/\beta$. Plates with $k_s < k_s^*$ are bent and support slightly smaller loads, while stiffer plates remain flat.

For plates much larger than the capillary length, $\beta \gg 1$, the force and torque balances become, respectively: $2\beta\mathcal{D} \approx \beta^2 \cos\alpha \sin\alpha$, and $4k_s\alpha + \mathcal{D}\beta^2 \cos\alpha \approx \frac{\beta^3}{3} \sin\alpha$, when $k_s \sim \mathcal{O}(\beta^3)$. The force and torque balances are now prescribed by the spring, the weight of the plate, and hydrostatic pressure. The configuration parameter H does not appear in the leading order terms for the force and torque balances of large plates, indicating that large plates are insensitive to surface tension. We return to Archimedes' principle: the plate load is maximized when the most fluid is displaced, or $\alpha = \pi/4$, as in Fig. 2. From the torque balance, the optimal stiffness associated with this configuration is $k_s^* = \beta^3/(12\sqrt{2}\pi)$ (Fig. 2(c)), for which the load is $\mathcal{D}_{\max} \sim \beta/4$ (Fig. 2(b)). When the plate is much larger than the plate edge depth H, the bulk of the fluid displaced is associated with the plate deformation rather than the meniscus, as shown in Fig. 3(b).

For any plate size, bending is advantageous if the plate size and tilt angle lies in the shaded region in Fig. 2(a), allowing the plate to bear a greater load than a flat plate. For plates on the order of a capillary length, $\beta \approx \mathcal{O}(1)$, both the hydrostatic pressure and surface tension are important in the force and torque balances. For these plates, the optimal bending angle is determined by the trade-off between fluid displaced by bending the plate and the narrowing of the fluid column displaced above the plate. Thus, as shown in Fig. 2(a), the optimal plate tilt angle lies between 0 and $\pi/4$, the optimal angles in the limiting cases of small and large plates, respectively.

We proceed by extending our results from a hinged to a continuously deformable plate. For small plates, we expect flat plates, at a depth of $\sqrt{2}\ell_c$, to support the greatest load since they displace the most fluid (as in Fig. 3(a)). We anticipate flexure to assist with weight-bearing for plates above a critical size. In the larger plate limit, we expect the optimal weight-bearing large plate shape to be that which displaces the most fluid, specifically, a semicircle.

For a continuously deformable plate of a given size, we search for the plate shape that minimizes the total energy while maximizing the plate load: max $\mathcal{D}$ s.t. $\delta\Pi = 0$. Components of potential energy for continuously deformable plates are a generalization of those developed in "Flotation of hinged plates" and can be written in integral form. Henceforth, EI is the bending stiffness per unit width of the plate so the elastocapillary length is $\ell_{ec}^2 = EI/\sigma$ and the dimensionless stiffness is Λ, as defined in Table I. We represent the shape of the continuous plate by its curvature, parameterized by the vector $\vec{c}$ with n elements. The principle of minimum potential energy results in a vertical

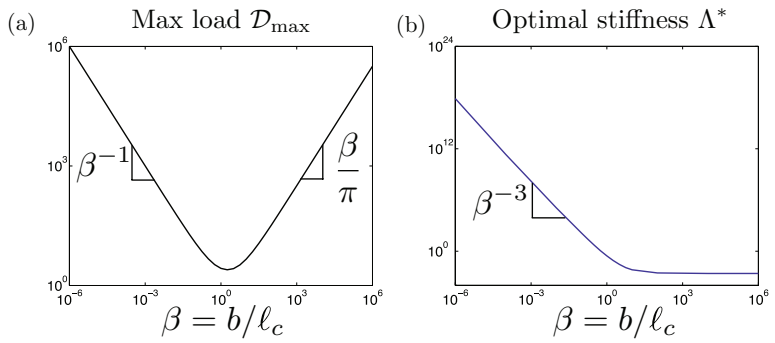

FIG. 4. (a) Maximum load as a function of dimensionless plate size, $\beta = b/\ell_c$ for a flexible plate. (b) Optimal bending stiffness Λ^* (specifically, that which bears the most weight) as a function of plate size. The optimal stiffness for large plates depends on size because the dominant terms in the force and torque balances are due to hydrostatic pressure while the weight of small plates is supported primarily by surface tension.

force balance and a torque balance, reducing the optimization problem to

$$\max_{H,\vec{c}} \ \mathcal{D}(\beta, \vec{c}, H, \Lambda),$$
$$\text{s.t. } \Sigma F(\beta, \vec{c}, H, k_s, \mathcal{D}) = 0, \ \ \Sigma \tau_i(\beta, \vec{c}, H, \Lambda, \mathcal{D}) = 0, \ \ i = 1, 2, ...n. \tag{12}$$

The problem is solved numerically using the MATLAB optimization toolbox. For small plates, the equilibrium plate shape that minimizes energy and maximizes density is a flat plate, and arises with bending stiffness as reflected in Fig. 4(b). As in "Flotation of hinged plates," the surface tension forces dominate and the flat plate supports the maximum load, $\mathcal{D}_{\max} \sim 1/\beta$, in this small plate limit (Fig. 4(a)).

The large plate shape that displaces the most fluid above the plate and supports the maximum density is necessarily a semicircle, an intuitively satisfying result confirmed by the numerical optimization. Increasing the stiffness or the elastocapillary length, Λ, is equivalent to increasing the energetic cost of bending. As a result, as Λ is increased progressively beyond the optimal stiffness Λ^*, the optimal plate shape is gradually less bent and displaces less liquid, as shown in Fig. 5(a) in the case of large plates, $Bo \gg 1$. We note that the plate at the optimal stiffness Λ^* is that which bears the greatest load, $\mathcal{D}_{\max} \sim \beta/\pi$ as illustrated in Fig. 4(a), and that this load decreases for any other Λ. The plate shapes in Fig. 5(a) resemble those presented by Reis *et al.*[5] for an elastic plate loaded at its midpoint.

For plates on the order of the capillary length, $Bo \sim 1$, both hydrostatic pressure and surface tension are important and the plate shape that displaces the most fluid is slightly bent, as shown in Fig. 5(b).

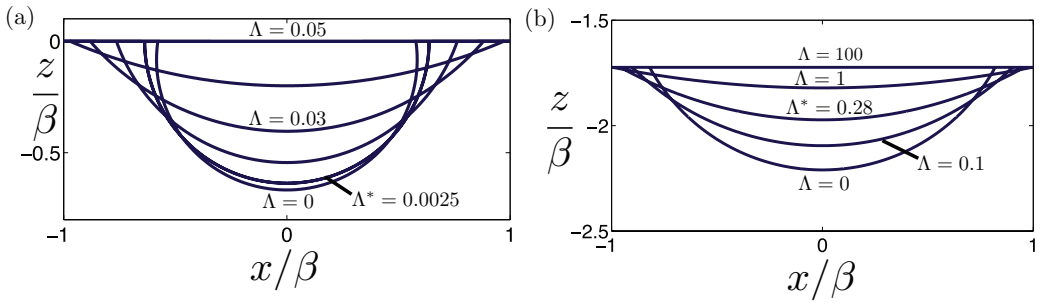

FIG. 5. (a) Plate shapes that maximize load for various stiffnesses, Λ, at large Bo ($\beta = 10^4$). The maximum load is achieved at the optimal stiffness $\Lambda^* = 0.025$. At this stiffness, the flexible plate displaces the most fluid, and so can support the greatest load. (b) Plate shapes that maximize load for various stiffnesses at $Bo \sim 1$ ($\beta = 1$). A slightly bent plate displaces the most fluid, and so supports the greatest load.

We have demonstrated that flexibility can assist in interfacial flotation for bodies on the order of the capillary length and larger. Consideration of the minimum total potential energy yielded force and torque balances whose form depended on body size. For plates much smaller than the capillary length, flat, rigid plates bear the most weight. Such small plates are supported predominately by capillary forces, thus plate bending results in a diminution of fluid displaced above the plate, as illustrated in Fig. 3(a), and so diminishes buoyancy.

Plates on the order of the capillary length displace the most fluid when flexible and slightly bent, as both hydrostatic pressure and capillary forces contribute to weight support. Compared to optimally flexible large or small plates, intermediate sized plates support the lowest plate density, as illustrated in Fig. 2(b).

A large plate supports a maximum load by deforming to $\alpha = \pi/4$ in the hinged case and to a semicircle in the continuous case, thereby displacing the maximum fluid volume, and minimizing the potential energy of the plate. Increasing plate stiffness increases the energetic cost of bending, forcing the plate to flatten (Fig. 5(a)), thus decreasing its load-bearing capacity.

Many water-walking insects are flexible and have length scales on the order of a capillary length.[3] At this scale, we have seen that bending allows an object to bear a greater load than if flat. To model raft-like structures and plants found in nature, we must generalize our theory to three dimensions. Nevertheless, our study does provide some insight for three-dimensional objects such as capillary rafts. Vella *et al.*[16] noted that capillary rafts comprised of many particles exhibit elastic behavior, and inferred effective values of the Young's modulus and Poisson ratio for rafts comprised of various materials, Similarly, Mlot *et al.*[8] inferred the effective constitutive properties of the ant raft. Our study indicates the manner in which flexibility assists the flotation of these rafts. Floating flexible biological organisms may deform in a variety of manners. Plants such as lily pads may buckle or experience out-of-plane folding. Films or membrane-like materials can stretch to withstand large loads, while the flowers of some aquatic plants may avoid buckling during submergence by having petals that overlap.[5]

Modeling more complex rheology and geometry, e.g., variable stiffness distribution along the plate, would be relatively straightforward using our approach. Comparison with data on the distribution of material stiffnesses and typical load cycles in various organisms would provide quantitative confirmation that water plants and floating colonies of interfacial creatures use flexibility to improve flotation.

The authors thank José Bico for helpful suggestions and the NSF-GRFP and Battelle Memorial Institute for financial support.

[1] T. L. Heath, *The Work of Archimedes* (Cambridge University Press, Cambridge, 1897).
[2] J. Keller, "Surface tension force on a partly submerged body," Phys. Fluids **10**, 3009–3010 (1998).
[3] J. W. M. Bush and D. Hu, "Walking on water: Biolocomotion at the interface," Annu. Rev. Fluid Mech. **38**, 339–369 (2006).
[4] T. A. McMahon and J. T. Bonner, *On Size and Life* (Scientific American Library, New York, 1983).
[5] P. Reis, J. Hure, S. Jung, J. W. M. Bush, and C. Clanet, "Grabbing water," Soft Matter **6**, 5705–5708 (2010).
[6] D. Vella, "The fluid mechanics of floating and sinking," Ph.D. dissertation (Trinity College, University of Cambridge, Cambridge, 2007).
[7] J. Voise, M. Schindler, J. Casas, and E. Raphael, "Capillary-based static self-assembly in higher organisms," J. R. Soc., Interface **8**, 1357–1366 (2011).
[8] N. Mlot, C. Tovey, and D. Hu, "Fire ants self-assemble into waterproof rafts to survive floods," Proc. Natl. Acad. Sci. U.S.A. **108**, 7669–7673 (2011).
[9] D. Vella, P. Metcalfe, and R. Whittaker, "Equilibrium conditions for the floating of multiple interfacial objects," J. Fluid Mech. **549**, 215–224 (2006).
[10] D. Vella, "Floating objects with finite resistance to bending," Langmuir **24**, 8701–8706 (2008).
[11] K. Park and H. Kim, "Bending of floating flexible legs," J. Fluid Mech. **610**, 381–390 (2008).
[12] X.-Y. Ji, J.-W. Wang, and X.-Q. Feng, "Role of flexibility in the water repellency of water strider legs: Theory and experiment," Phys. Rev. E **85**, 021607 (2012).
[13] Q.-S. Zheng, Y. Yu, and X.-Q. Feng, "The role of adaptive-deformation of water strider leg in its walking on water," J. Adhes. Sci. Technol. **23**, 493–501 (2009).
[14] J. Liu, X. Feng, and G. Wang, "Buoyant force and sinking conditions of a hydrophobic thin rod floating on water," Phys. Rev. E **76**, 066103 (2007).
[15] J. N. Reddy, *Energy Principles and Variational Methods in Applied Mechanics* (Wiley-Interscience, Hoboken, 2002).
[16] D. Vella, P. Aussillous, and L. Mahadevan, "Elasticity of an interfacial particle raft," Europhys. Lett. **68**, 212–218 (2004).